Journal of Marine Research, 45, 843–870, 1987

Accurately monitoring the Florida Current with motionally induced voltages

by Peter Spain[1] and Thomas B. Sanford[1]

ABSTRACT

A new experimental technique for appraising how accurately submarine-cable (subcable) voltages monitor oceanic volume transport is presented and then used to study voltages induced by the northern Florida Current. Until recently, subcable voltages have been largely dismissed as an oceanographic tool because their interpretation can be ambiguous. They depend upon the transport field, the electrical conductance of the environment, and the mutual spatial distribution of these two quantities. To examine how these three factors affect subcable voltages at a particular site, we combine data from two different velocity profilers: XCP and PEGASUS. These instruments provide vertical profiles of velocity, temperature, and motionally induced voltage at several sites across a transect. From this information, we determine if and why subcable voltages track volume transport. We conclude that subcable voltages measured in the northern Florida Straits accurately monitor the Florida Current transport because they are insensitive to the spatial distribution of the flow—a result that stems from a large and rather uniform seabed conductance. Subcable voltages should be reconsidered for oceanic monitoring elsewhere because the validity of their interpretation can now be assessed.

1. Introduction

Significant fluctuations in volume transport accompany the seasonal and interannual variability of many oceanic phenomena. Some examples include the annual reversal of the Somali Current in response to the transition of the monsoons (Leetmaa *et al.,* 1980), the interannual movement of the Kuroshio between its bimodal paths (Taft, 1972), and the attenuation of the Pacific equatorial undercurrent during an El Niño (Firing *et al.,* 1983). Moreover, fluctuations in the transport of major currents affect air-sea interaction, fisheries management, and probably climate. To study oceanic phenomena exhibiting seasonal and interannual variability, long records of ocean currents are needed; yet, conventional instruments, such as current meters and velocity profilers, are not suitable for continuously measuring volume transport over many years.

In contrast, submarine-cable (subcable) voltages, which can be used to measure ocean currents indirectly, have accurately measured the variability of the Florida

1. Applied Physics Laboratory and School of Oceanography, University of Washington, Seattle, Washington, 98105, U.S.A.

Current since 1969 (Sanford, 1982). During 1982–1983, the accuracy of those measurements was established via a long-term calibration program in the northern Florida Straits (Larsen and Sanford, 1985). Subcable voltages were compared with concurrent transport measurements derived from PEGASUS, an acoustically-tracked current profiler (Spain *et al.*, 1981). This intercomparison found that voltages closely tracked the volume of water transported through the northern Florida Straits.

Prior to that study, subcable voltages had been largely dismissed as an oceanographic tool because their interpretation can be ambiguous and the instrumentation was unavailable to calibrate the voltages accurately. While Larsen and Sanford's (1985) approach solved the latter aspect of this problem, their calibration was philosophically similar to earlier empirical studies that used data from moored current meters or current meters lowered from ships (Teramoto, 1971; Bowden and Hughes, 1961). Any empirical calibration of subcable voltages is limited by two drawbacks when the ambiguity of the voltage interpretation is addressed. The robustness of the voltage calibration can only be evaluated by obtaining a long time-series of transport measurements with concurrent subcable voltage data. Even more important, the empirical calibrations do not elucidate *why* voltages track transport.

In this paper, we describe and apply a simple experimental technique that avoids these drawbacks. Using an approach that has a similar goal but dissimilar methodology to Teramoto's (1971), we evaluate the geophysical factors affecting subcable voltages in the northern Florida Straits: the transport field, the environmental electrical conductance, and their mutual spatial distributions. The role of these various influences on subcable voltages can be assessed by combining vertical profiles of velocity, temperature, and motionally induced voltage that have been measured along a transect. After analyzing these data, we understand how subcable voltages are constituted, calibrate the voltages in terms of transport, and evaluate how accurately transport can be monitored with this calibration if the ocean current meanders.

When our experimental technique was applied near the subcable calibrated by Larsen and Sanford (1985), three key results were obtained.

- Subcable voltages accurately track Florida Current transport at this site because they depend predominantly on the transport magnitude and only weakly on its distribution.
- Our transport-voltage calibration for the northern Florida Current matches what Larsen and Sanford found with their long-term empirical calibration.
- The voltage calibration is fairly insensitive to meandering of the Florida Current because seabed conductance is large and rather uniform, thereby weakening the voltage dependence on the form of the flow.

Based on these results from the Florida Current, we conclude that it is now possible to determine whether an unambiguous transport signal can be extracted from subcable

voltages at a particular site. In this light, they should be reconsidered as a tool for long-term monitoring of oceanic transport at critical locations.

In the following sections, we review the history of monitoring the Florida Current with subcable voltages, introduce some of the theory of subcable voltages, and construct an analytical model connecting them to transport. We then turn to our observational study of the voltages induced by the northern Florida Current. After describing our experimental technique, we report and interpret results from the observational program. Finally, conclusions from this study are discussed.

2. Background

Three phases in the history of monitoring the Florida Current with subcable voltages are summarized: what originally motivated their use, why they were discredited, and what new evidence supports the method.

a. Original motivation. Measuring ocean currents with subcable voltages stems from Faraday's Law. According to this law, an electric field will be induced when seawater moves through the geomagnetic field. The voltage associated with the induced electric field can be measured with two electrodes interconnected through a voltmeter by a submarine cable—hence the name, subcable voltages. Because of the high electrical conductivity of seawater, the ocean acts as a low impedance electromotive source. Voltages observed with subcables over an electrically conducting seabed, however, are less than the generated, or open-circuit, values. This attenuation, or "shorting," arises because the finite conductance of the seabed provides a return circuit for electric current and some of the generated voltage is "dropped" as the electric current passes through the seawater. If electric current also circulates in the horizontal plane (Sanford, 1971; Chave and Cox, 1982), this difference between the observed and the generated voltages will be modified. A lucid, theoretical account of motionally induced voltages in the sea is presented in the seminal paper by Longuet-Higgins *et al.* (1954).

Conclusions from theoretical models motivated the first attempts to monitor ocean currents with subcable voltages. Two key simplifying assumptions were made in these models: water depth and electrical conductances (seawater and seabed) were both assumed to be horizontally uniform. As a result, the motionally induced voltage should be *linearly* related to the volume of water transported by the ocean current (Malkus and Stern, 1952). But the two assumptions underpinning this conclusion were not valid where early measurements were made; the interpretation of the measurements was equivocal.

b. Ambiguous interpretation of measurements. The first measurements of the voltage induced by the Florida Current were initiated by Henry Stommel in 1952 and continued for a decade. During this period, the voltage between Key West, Florida,

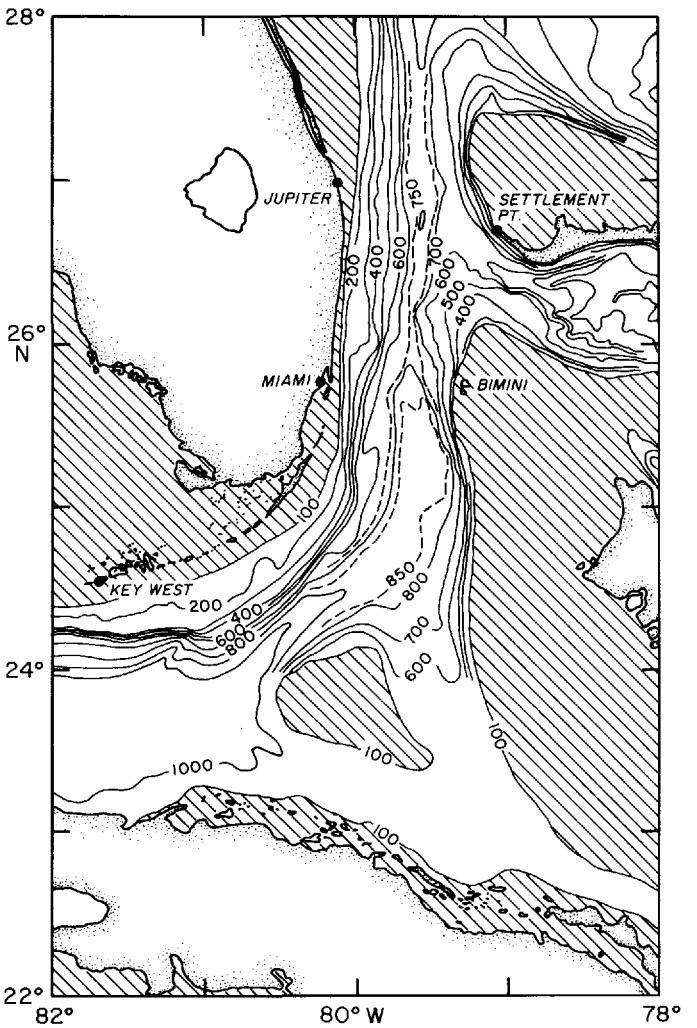

Figure 1. Chart of measurement location and bottom topography (in meters). The profiling measurements described in the paper were made in the northern Florida Straits, east of Jupiter.

(Fig. 1) and Havana, Cuba, was monitored and related to transport, but it was never calibrated. These data contained some unusual features that were thought to be caused by large, abrupt ("catastrophic") transport fluctuations (Wertheim, 1954; Stommel, 1956, 1965). However, when these results were compared with direct transport measurements made 10 years later (Schmitz and Richardson, 1968), there were two significant differences: the annual mean value for volume transport inferred from the voltages was low, and "catastrophic" transport fluctuations were not observed.

Because of these differences, subcable voltages were largely abandoned for oceanographic studies. What caused such disparity between observations?

As noted earlier, the subcable voltage is less than the generated (open-circuit) voltage wherever the seabed is conductive. Unless the "missing" voltage is compensated by an adjustment factor in the transport-voltage calibration, transports inferred from the subcable voltage will be low. The small value for the annual mean in the Key West transport data could have been corrected by making calibration measurements.

On the other hand, "catastrophic" fluctuations in the Key West voltage data could not be easily corrected. The interpretation of any change in subcable voltage is ambiguous if, as in the general case, subcable voltages are sensitive to both the magnitude and the spatial distribution of the transport. Large fluctuations in the Key West voltage data were attributed to meandering of the Florida Current because similar changes had not been seen when transport was measured directly (Schmitz and Richardson, 1968). But simultaneous measurements of transport and voltage were not available to verify this notion. Interest in extracting oceanographic signals from subcable voltages waned until the Florida Current was to be monitored for climate studies.

c. New results. In 1981, the Subtropical Atlantic Climate Study—STACS (Molinari *et al.*, 1985)—began simultaneously measuring Florida Current transport and subcable voltages across the northern Florida Straits. Three important results from this study pertain to earlier work:

- The voltages in the northern Florida Straits are linearly related to Florida Current transport (Larsen and Sanford, 1985).
- Large, abrupt changes in transport (e.g., 10 sverdrups in 1 week) were simultaneously observed with subcable voltages, PEGASUS, and current meters (Lee *et al.*, 1985). Similar transport fluctuations have also been observed with PEGASUS farther downstream (Halkin and Rossby, 1985).
- Transport events of long duration, seen before in old subcable data (Sanford, 1982), were recorded with subcable voltages and current meters (Lee *et al.*, 1985).

These new results from STACS demonstrate the oceanographic utility of subcable voltages, particularly for observing low frequency variability. Places do exist where the data can be interpreted unambiguously. Although subcable voltages at Key West may be sensitive to the form of the Florida Current south of the keys, the STACS results suggest that the voltage-transport relationship there is not as nonlinear as first thought. Indeed, much of the variability in the old data (Stommel, 1956) has similar magnitude to what was observed in STACS.

In summary, subcable voltages can be difficult to interpret because the voltage-

transport relationship is inherently nonlinear. Yet, at some sites voltages accurately track transport. In the following sections, a new experimental technique is presented that helps determine whether a proposed measurement site is appropriate for subcable measurements.

3. Motional induction in the sea

Variables and concepts that will be used throughout the paper are now introduced. The key ideas from this discussion are that for situations often encountered in the ocean the induced electric field is independent of depth and is the same as if the water moved with a velocity $\bar{\mathbf{v}}^*$, which is proportional to the depth-averaged velocity ($\bar{\mathbf{v}}$). However, nonlinearity enters when this relationship is extended to subcable voltages and volume transport. The effects of this nonlinearity need to be quantified if transport is to be monitored accurately with subcable voltages.

a. Basic concepts. The electric field ($-\nabla\phi$) and electric current density ($\mathbf{J}$) generated by movement through a quasi-steady geomagnetic field ($\mathbf{F}$) are related to the velocity field ($\mathbf{v}$) by Ohm's law for a moving medium of electrical conductivity (σ). The present discussion is restricted to flows in which vertical motions are negligible so that the east (x) component of this equation can be written

$$\frac{\partial\phi}{\partial x} = F_z v - \frac{J_x}{\sigma}, \tag{1}$$

where v is northward flow, F_z is the vertical (z) component of the earth's magnetic field, and $\partial\phi/\partial x$ is the eastward gradient of the potential difference that would be measured with stationary electrodes separated horizontally along an east/west line.

The vertical integral of (1) is used to interpret subcable voltages in terms of transport, but two key assumptions need to be valid for accurate results.

- The horizontal potential gradient, which is measured at the seafloor, is assumed to be the same for all levels between the base of the conducting seabed (H_s) and the sea surface.
- The circulation of the induced electric currents is assumed to satisfy

$$\int_{-H_s}^{0} J_x \, dz = 0.$$

These two assumptions are considered in turn. Provided an ocean current, which may be highly baroclinic, has a width greatly exceeding its depth, induced electric currents will be almost entirely horizontal at every depth. In this situation, which can be modeled by a set of batteries connected in parallel, the value of the horizontal potential gradient at some depth $z = -\xi$ should be identical to the value at the seafloor

as long as

$$\frac{\partial}{\partial x}\int_{-H}^{-\xi} F_H u \, dz$$

remains small (Sanford *et al.*, 1978); u is east flow, F_H is the horizontal component of the earth's magnetic field, and H is the water depth.

The second key assumption requires that depth-independent electric currents be negligible. This constraint should hold if downstream variations of the flow field are slight so that electric currents do not circulate in horizontal loops and, second, if there are no depth-independent electric currents that have been generated by external sources (Sanford and Flick, 1975).

When (1) is vertically integrated from the base of the conducting seabed to the sea surface, and the preceding assumptions are used, the result can be written as

$$\frac{\partial \phi}{\partial x} = F_z \frac{\int_{-H}^{0} \sigma v \, dz}{\int_{-H_s}^{0} \sigma \, dz}. \tag{2}$$

Eq. (2) states that the eastward potential gradient, measured with stationary electrodes at any depth, is proportional to a conductivity-weighted vertical integral of northward velocity.

Following Sanford (1971), define

$$\frac{\int_{-H}^{0} \sigma v \, dz}{\int_{-H_s}^{0} \sigma \, dz} = \bar{v}^*,$$

where the overbar indicates an average over the water depth. Eq. (2) can now be interpreted as stating that the observed eastward potential gradient is the same as if the ocean current moved with a northward barotropic velocity, $\bar{v}^*$. In the deep ocean, observations show that $\bar{v}^*$ mirrors the vertically averaged velocity ($\bar{v}$) with an error of about 10% (Sanford *et al.*, 1985). Their interrelation follows from the definition of $\bar{v}^*$.

$$\bar{v}^* = \frac{\overline{\sigma v}}{\bar{\sigma}\bar{v}(1 + \lambda)} \bar{v}. \tag{3}$$

The symbol λ denotes the ratio of the seabed ($\int_{-H_s}^{-H} \sigma \, dz$) and water column ($\int_{-H}^{0} \sigma \, dz$) electrical conductances. Even though the electrical conductance of the seabed may be invariant, λ can be much larger in shallow water than in deep water; in contrast to the deep ocean, $\bar{v}$ can therefore greatly exceed $\bar{v}^*$ in shallow water (Sanford and Flick, 1975).

A relation between $\bar{v}^*$ and transport/unit width (t) is defined by introducing an equivalent water depth (H_e).

$$\bar{v}^* H_e = \bar{v} H = t. \tag{4}$$

A physical interpretation of H_e follows when (3) and (4) are combined to show that

$$H_e = H(1 + \lambda)\, \overline{\sigma v}/\overline{\sigma v}.$$

The electrical conductance of the seabed can be modeled as a motionless layer of seawater with depth λH overlying a nonconducting seabed. A superposition of the observed seawater column and such a motionless layer would have a depth of $H(1 + \lambda)$ and the same total conductance as the observed environment. The factor $\overline{\sigma v}/\overline{\sigma v}$ is generally within 10% of unity. Thus for a nonconducting seafloor, H_e is approximately H, whereas for a highly conducting seafloor, H_e is much larger than H.

b. Subcable voltages. Voltages ($\triangle\phi$) recorded on a subcable that is oriented east/west can be expressed as the lateral integral of (2), which after substituting (3) and (4) becomes

$$\frac{\triangle\phi}{F_z} = \int_0^L \frac{t}{H_e}\, dx, \tag{5}$$

where F_z is assumed to be invariant along the line of integration. The integration includes transport across the cable between two electrodes, which are horizontally separated by a distance L. In many applications, this distance spans a strait.

Subcable voltages and volume transport (T) can be explicitly related by using a Reynolds decomposition on the right-hand side of (5). Horizontal averages and deviations are identified by the $\langle\ \rangle$ and $'$ signs, respectively. After a binomial expansion is applied, (5) becomes

$$\frac{\triangle\phi}{F_z} = \frac{T}{\langle H_e \rangle} - \frac{\langle t' H_e' \rangle L}{\langle H_e \rangle^2} + O\left(\frac{H_e'}{\langle H_e \rangle}\right)^2.$$

Factors affecting the magnitude and linearity of the voltages are more apparent if higher order terms are ignored so that

$$\frac{\triangle\phi}{F_z} = \underset{\text{(a)}}{\frac{T}{\langle H_e \rangle}} \underset{\text{(b)}}{\left[1 - \frac{\langle t' H_e' \rangle}{\langle H_e \rangle \langle t \rangle}\right]}. \tag{6}$$

Eq. (6) shows that voltages depend not only upon the magnitudes of the volume transport and the environmental electrical conductance (term (a)), but also upon their mutual spatial distributions (term (b)). A key point to note for understanding (6) is that terms (a) and (b) are both inversely related to $\langle H_e \rangle$. Accordingly, large values of

$\langle H_e \rangle$ will enhance the linearity of the $\Delta\phi - T$ relationship because the nonlinear part of $\Delta\phi$, which is the product of (a) and (b), has a quadratic dependence on $\langle H_e \rangle$. This enhanced linearity is gained, however, at the expense of decreased voltage magnitude (term (a)). Except where t and H_e are uncorrelated, a natural tradeoff will therefore exist between the voltage magnitude and the linearity of the transport-voltage relation. Evaluating this tradeoff is the key to understanding whether fluctuations in subcable voltages reflect transport variability.

In the sections that follow, the parameters of (6) are derived from the velocity profiles collected in the Florida Current, and the reasons why subcable voltages track the Florida Current at 27N are explained.

4. Method and measurements

Before ocean transports can be accurately monitored with subcable voltages, both the voltage attenuation caused by the conducting seabed and the sensitivity of the voltages to the form of the flow field must be evaluated. Seabed "shorting" has traditionally been evaluated from the slope of a linear regression between simultaneous measurements of subcable voltages and volume transport.

Here we use a new approach that combines data from two velocity profilers, PEGASUS and XCP, to measure the transport and electrical conductances at several sites along a transect. Both the seabed "shorting" and the nonlinearity of the voltages can be evaluated explicitly from these data.

a. Experimental technique. A vertical profile of current velocity can be obtained by differentiating the trajectory of a probe that falls freely from the surface to the seafloor (Rossby, 1969). The profiler trajectory is obtained by acoustically tracking the instrument relative to a bottom-mounted reference frame. PEGASUS, developed by H.T. Rossby, is based on this idea (Spain *et al.*, 1981). Both t and $\bar{v}$ are derived from the vertical integral of the northward component of the current profile, $v(z)$. PEGASUS also records a vertical profile of temperature which can be converted to conductivity by using a conductivity-temperature relation obtained from local hydrographic or CTD data.

In (1), the gradient of the potential difference observed with stationary electrodes is composed of two parts. If the electrodes are advected horizontally with the local flow, the first part ($F_z v$) is canceled by an equal and opposite potential gradient in the electrode line (Longuet-Higgins *et al.*, 1954). An analysis by Sanford (1971) showed how measurements of $\mathbf{J}/\sigma$, the second part of (1), reveal the depth dependent, or baroclinic, portion of a current. Thus a freely falling instrument that measures $\mathbf{J}/\sigma$ records a vertical profile of relative velocity. The Sippican expendable current profiler, XCP, formerly called the XTVP (Sanford *et al.*, 1981) is this type of instrument.

The vertical profile recorded by the XCP is $v(z) - \tilde{v}$, where $\tilde{v}$ is a velocity incorporating several depth-independent contributions: $\bar{v}^*$, a velocity proportional to $\bar{v}$;

$\hat{\mathbf{v}}$, a velocity related to local electric fields that are generated by "remote" flow and other external geophysical effects; and ϵ_I, instrument errors. For our purposes, the latter two contributions are "noise." For comparison, these same three contributions are measured by stationary electrodes, although the instrument errors will not be the same. If $\hat{\mathbf{v}}$ and ϵ_I are negligible, the voltage observed with stationary electrodes will be related to just $\bar{\mathbf{v}}^*$, which reflects the barotropic portion of a current.

Based on this idea that *moving* electrodes reveal the depth-dependent flow and *stationary* electrodes reveal the depth-independent flow, one can see that by combining these two types of measurements the profile of total flow can be estimated. Our new experimental technique reverses this logic. By computing the difference between a PEGASUS profile of total velocity and an XCP profile of relative velocity, we measure $\tilde{\mathbf{v}}$. Our signal ($\bar{v}^*$) is extracted from the northward component of $\tilde{\mathbf{v}}$ by finding the part that varies directly with $\bar{v}$. The "local" contribution to (5) can then be found by multiplying $\bar{v}^*$ by both the width it characterizes and F_z. The subcable voltage can therefore be synthesized by measuring the simultaneous profiles at a number of sites along a transect.

An advantage of this new approach is that any spatial structure in the relationship between transport and motionally induced voltage can be seen. Observing such structure helps in understanding how the subcable voltages are constituted and how they will vary if the transport distribution changes. In contrast, empirical calibrations compare subcable voltages with local current measurements. This intercomparison must include a variety of the forms taken by the flow to assess whether voltage fluctuations can be confidently attributed to transport magnitude changes. Unlike the new method, this assessment process requires a long-term calibration program.

We now turn to the mechanics of quantifying and appraising the relationship between $\triangle\phi$ and T. The equivalent depth (H_e) at each site is defined to be positive and obtained from $\bar{v}^*$ and t using (4). After lateral averages and deviations of t and H_e are computed, a calibration relation for $\triangle\phi$ and T is produced with (6). To understand this relation, the conductance ratio (λ) is evaluated at each site using (3) and seawater conductance is derived from PEGASUS temperature profiles. The seabed conductance is then computed as the product of λ and seawater conductance. At this point, the information needed to evaluate and to understand both the seabed "shorting" and the nonlinearity of the subcable voltages is available.

b. Observational program. Data for evaluating how the Florida Current affects motionally induced voltages were collected in the northern Florida Straits. Observations were made at 27N, near the submarine cable between Jupiter Inlet, Florida, and Settlement Point, Grand Bahama Island (Fig. 2). Eight velocity profiling stations formed a transect across the Florida Current; in mid-stream, the transect was several kilometers to the north of the subcable. Measurements were also made at two stations farther upstream to see how spatially representative the results at 27N were. The ninth

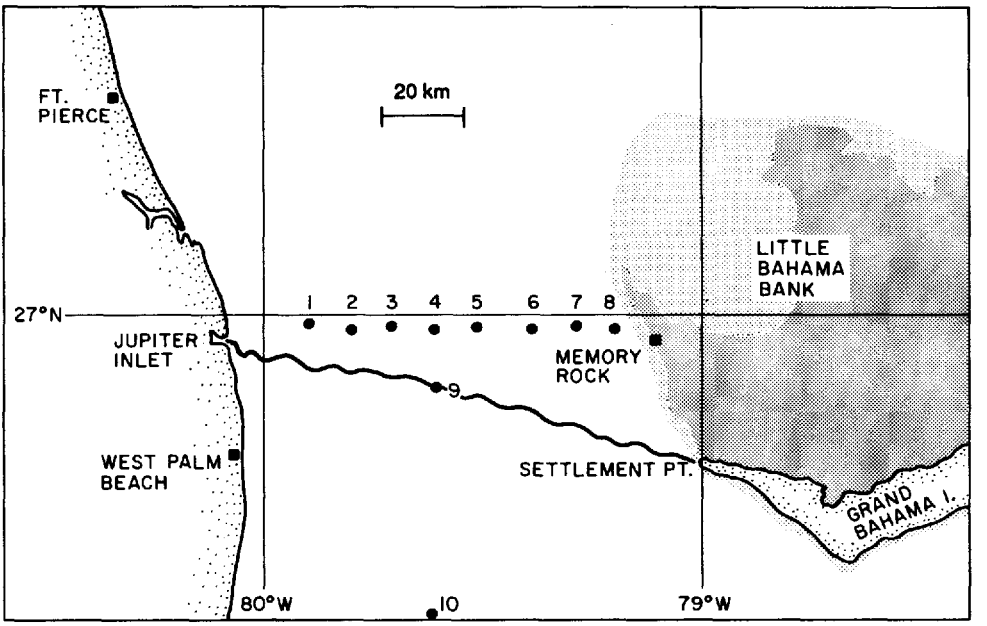

Figure 2. Chart of velocity profiling stations. The ten sites of simultaneous XCP and PEGASUS profiles are shown here, together with the line of the submarine cable between Jupiter Inlet, Florida, and Settlement Point, Grand Bahama Island.

profiling station was at the subcable, while the tenth was at 26.5N; both stations were in mid-stream and in deep water.

Most of the data were collected in one cruise (June 1982), aboard NOAA ship *Researcher,* when three transects of profile pairs were obtained. Some extra profiles were also taken at a few sites along the transect, to improve the data set, and at the station on the subcable. During a second cruise (Dec. 1983), *Researcher* met USNS *Lynch* at several profiling sites. PEGASUS was deployed from *Researcher,* and XCPs were launched from *Lynch.* Several profiles were measured at station 10 (26.5N), and more profiles were taken at the peripheral stations on the transect where measurement variability had been largest during the earlier cruise.

5. Data reduction

a. Data preprocessing. The velocity profiles were interpolated to a common, uniform depth grid. Only the north (magnetic) component of velocity was analyzed. XCP velocity components were relative to geomagnetic coordinates and had data spaced at 2.5 m intervals. Profiles were smoothed over 12 m by a Gaussian filter. After PEGASUS profiles had been rotated by 3.5° counterclockwise to be in geomagnetic coordinates, they were smoothed and interpolated as the XCP profiles had been.

PEGASUS temperature profiles were converted to conductivity via a linear regression based on CTD profiles obtained at the start of the cruise.

Overall, patterns of finestructure in the PEGASUS and XCP profiles were very similar. Some of the finestructure discrepancies (e.g., near the surface) result from real space-time differences because the ship was drifting in strong currents and the XCPs were generally launched about 10–15 minutes after PEGASUS. These errors were severe in shallow water where the velocity shear was enormous. Measurement errors were larger there, too. For example, signal dropout in the acoustic tracking records of PEGASUS was most severe at site 1; contamination of XCP profiles is largest in shallow water because any electric currents generated by external sources are amplified there.

Although patterns of finestructure were similar, features were not at identical depths in both profiles. XCP depths are calculated from elapsed times, whereas PEGASUS depths are determined from a pressure transducer. Depth differences were estimated by computing structure functions over 250 m intervals, and the XCP profiles were shifted down to align finestructure with corresponding features in the PEGASUS profiles. For the most part, the adjustment was slightly greater at depth. A typical value for the depth shift was 12 m (two data points), while its maximum was 24 m.

b. Data processing. Once the finestructure was aligned in the simultaneous profiles, the offset between the PEGASUS and XCP speeds was computed at all depths. At any level, this offset is an estimate of $\tilde{v}$ (Fig. 3). Depth-dependent measurement errors and higher order terms in $\partial\phi/\partial x$ produce the nonconstancy of $\tilde{v}$ that can be seen in Figure 3. The offset between the two profiles was linearly regressed against depth. The value of the offset at a depth equal to half the water depth was calculated and assigned to $\tilde{v}$; rms errors for these regressions were typically 2–3 cm/s, which corresponds to fractional errors of 5–10%.

If extraneous electric currents were negligible and instrument errors were insignificant, $\tilde{v}$ should equal $\bar{v}^*$ and be directly proportional to $\bar{v}$. Based on this idea, $\tilde{v}$ was linearly regressed against $\bar{v}$ to look for any contribution that did not depend on "local" flow. An intercept of +8 cm/s was found. The XCP measurement is thought to be biased by about +10 cm/s at 27N because water entrained in the probe's boundary layer produces a weak signal that is not included in real-time compensation for the fall rate of the probe. The intercept was attributed to this error and removed from $\tilde{v}$. The adjusted values of $\tilde{v}$ were called $\bar{v}^*$ and are plotted against $\bar{v}$ in Figure 4.

The quality of the $\bar{v}^*$ data was verified by an independent check based on (5) that used voltages from the nearby subcable (Fig. 2). The subcable, which was used by Larsen and Sanford (1985), extends from its broken end about 10 km off Jupiter Inlet to Settlement Point. For each of the three transects of simultaneous velocity profiles, the lateral integral of $\bar{v}^*$ was multiplied by F_z (0.42 10^{-4} T) and compared with the mean subcable voltage measured during the time taken to complete the transect. The

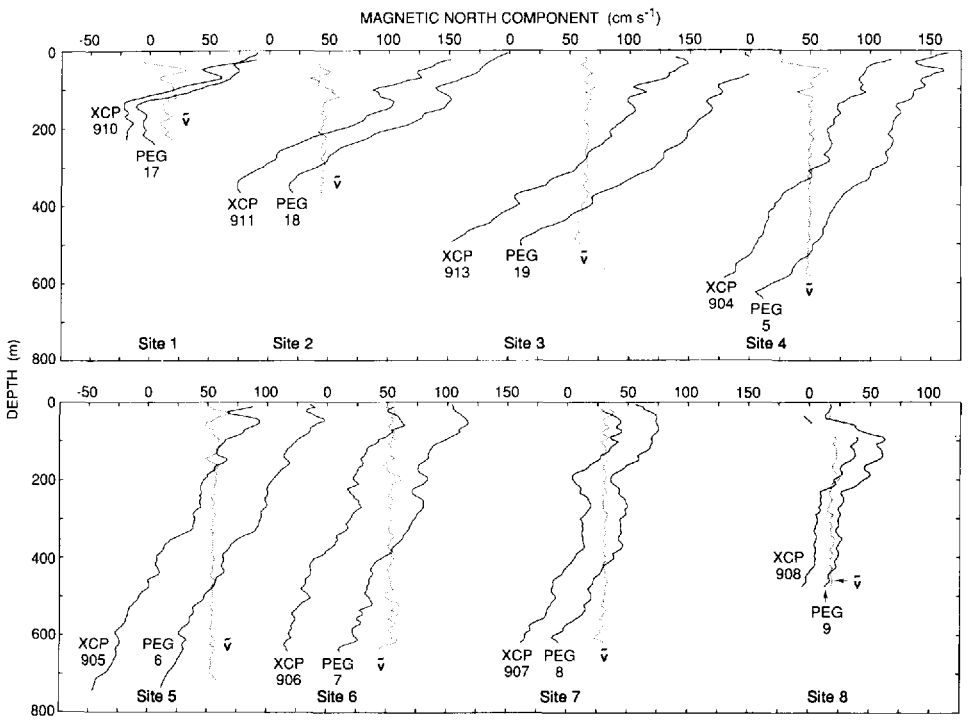

Figure 3. XCP and PEGASUS profiles and $\bar{v}$. Profiles from two measurement transects are shown here. The data at sites 1–3 were recorded during the second transect, while sites 4–8 come from the first transect. The composite transect is used because the data from sites 1–3 during the first transect were either missing or very noisy. The north (magnetic) component of flow is shown for each profiler. The dotted line is their difference which in the absence of measurement errors and higher order terms in $\partial\phi/\partial x$ would be depth invariant and equal to $\bar{v}$. The XCP data have been shifted down in depth to match the PEGASUS finestructure.

subcable integrals reflect a greater width than the 73 km included in the lateral integrals of $F_z\,\bar{v}^*$; thus, one should expect the subcable voltages to be larger.

Transect	1	2	3
Cable (V)	1.02	1.19	1.41
$F_z\int \bar{v}^*\,dx$ (V)	1.01	1.08	1.16

No profiles were taken in the shallow water regions at either end of the transect. If nearshore voltages do not greatly exceed values observed at the peripheral stations, the signal "missing" in the integrals is probably less than 60 mV.

The $\bar{v}^*$ data were combined with PEGASUS data to estimate λ with (3) and the equivalent water depth H_e with (4). Seabed conductance was estimated by the product

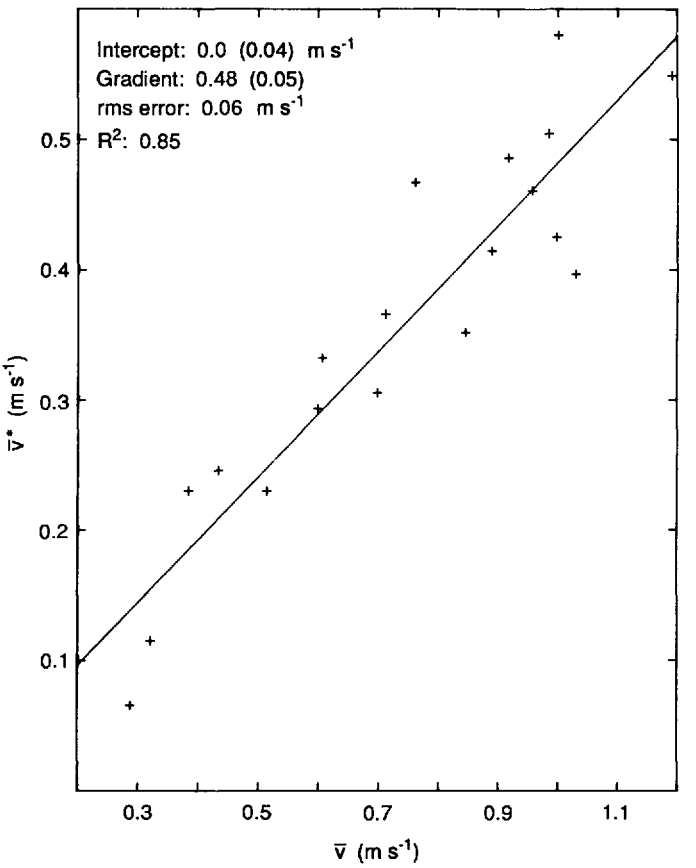

Figure 4. Simple linear regression between $\bar{v}^*$ and $\bar{v}$. The $\bar{v}^*$ and $\bar{v}$ values derived from data taken along the transect at 27N in the Florida Straits are intercompared and the best-fit line is drawn through the data. Only profiles in which the data return exceeded 80% are included. Statistics for the regression are shown, with the standard error for each of the regression parameters in parentheses.

$\lambda\,\bar{\sigma}\,H$, once $\bar{\sigma}$ had been derived from the PEGASUS temperature profile. The error of these seabed conductances is about 10%. The H_e and t data were combined to form $\langle t'\,H_e'\rangle/\langle H_e\rangle\langle t\rangle$ for each of the three measurement transects. Lateral averages were calculated by using the median value at each site, weighted by its station width. Median values were selected to produce statistics that were not biased by the few wild points recorded in shallow water.

6. Results

The new experimental approach evaluates both the magnitude and the spatial structure of H_e. Combining this information with similar information about t, one can

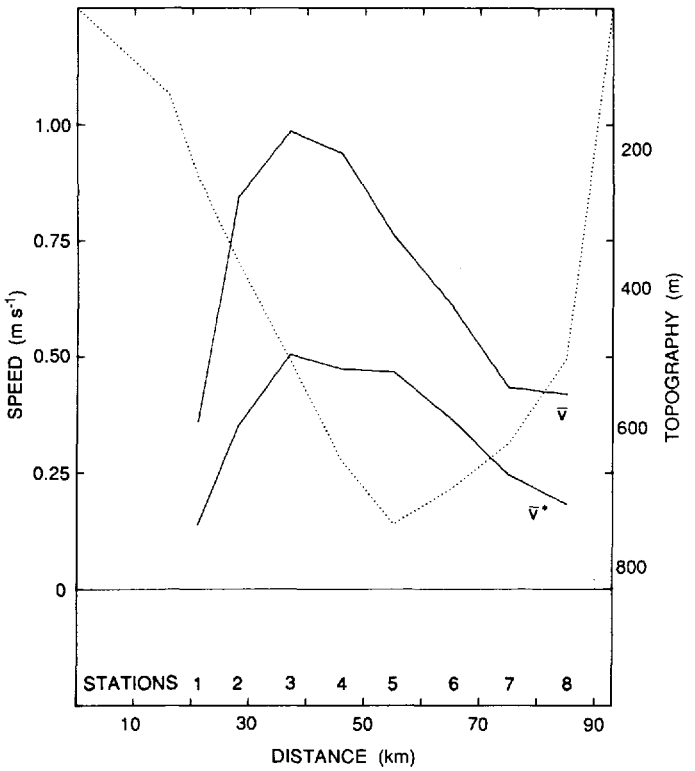

Figure 5. Transects of $\bar{v}$ and $\bar{v}^*$. The smaller magnitude and the eastward shift that distinguishes transects of $\bar{v}^*$ from those of $\bar{v}$ are apparent in this figure. The median of the observed values at each site is shown. The station positions are marked and their depths are joined by the dotted line.

generate a $T - \Delta\phi$ calibration that can then be analyzed for its linearity, accuracy, and sensitivity to changes in the form of the flow. An improved understanding of these aspects of the calibration follows from first examining the spatial distribution and interrelationship of its constituents.

a. Spatial characteristics. Two important differences distinguish transects of $\bar{v}^*$ from those of $\bar{v}$. Looking at Figure 5, which displays characteristic transects generated from median values at each site, one can see that the magnitude of $\bar{v}^*$ is typically about half that of $\bar{v}$, and second, the core of the $\bar{v}^*$ pattern is found in deeper water. The smaller magnitude of $\bar{v}^*$ arises because $(1 + \lambda)$ and $\overline{\sigma v}/\bar{\sigma}\bar{v}$ have unequal effects (see (3)). Figure 6 shows transects of these two factors. On average, the conducting seabed diminishes the ratio of $\bar{v}^*$ and $\bar{v}$ by about 55%, swamping the 10% amplification due to the speed-conductivity covariance. The different spatial character of $\bar{v}^*$ compared with $\bar{v}$ arises because the dominant factor $(1 + \lambda)$ varies inversely with water depth.

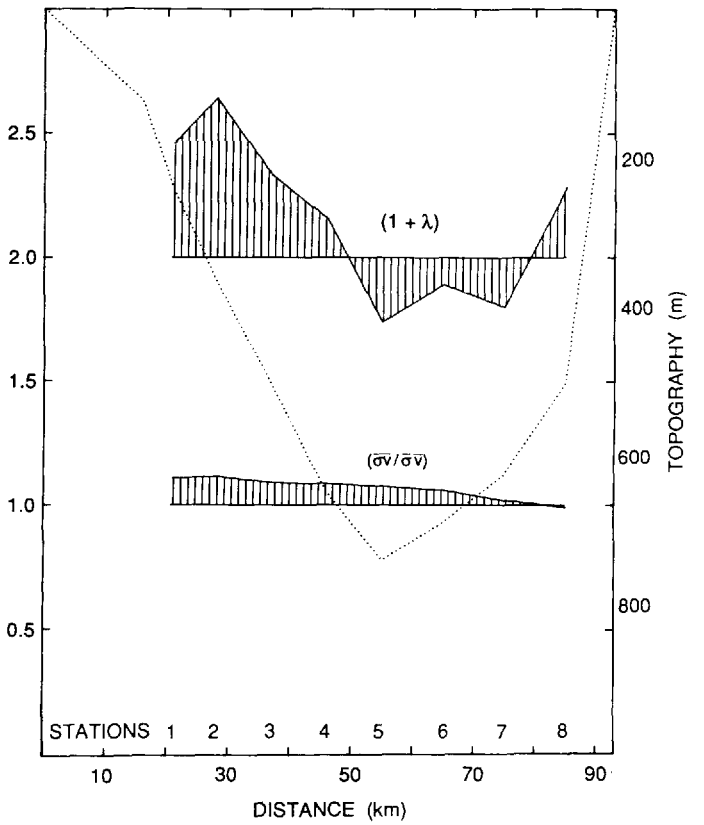

Figure 6. Transects of $(1 + \lambda)$ and $\overline{\sigma v}/\overline{\sigma}\,\overline{v}$. The two factors affecting the ratio of $\overline{v}$ and $\overline{v}^*$ are contrasted here. $(1 + \lambda)$ would be equal to 2 if the seabed and seawater conductances were identical, and would be equal to 1 over an insulating seafloor. $\overline{\sigma v}/\overline{\sigma}\,\overline{v}$ would be equal to 1 if speed and conductivity were not correlated. The median of the observed values at each site is shown. The shading emphasizes the different spatial dependence of each variable. Note the inverse dependence of $(1 + \lambda)$ on water depth.

The variability displayed by $(1 + \lambda)$ results from the varying ratio of seabed and seawater electrical conductances across the transect. Although the two conductances are similar for most of the transect (Fig. 7), seawater conductance rapidly decreases as the water shoals, thereby inflating λ. In contrast to this spatial variation in λ, seabed conductance itself is rather uniform, which governs the difference between H_e and H (Fig. 8). For this highly conducting seabed, H_e is typically about twice H, whereas for a poorly conducting seabed they would be nearly equal. Eastward of site 2, H_e is more uniform than H, having a coefficient of variation of 6%, about one third that of the water depth. If H_e were level, volume transport and subcable voltage would be uniquely related.

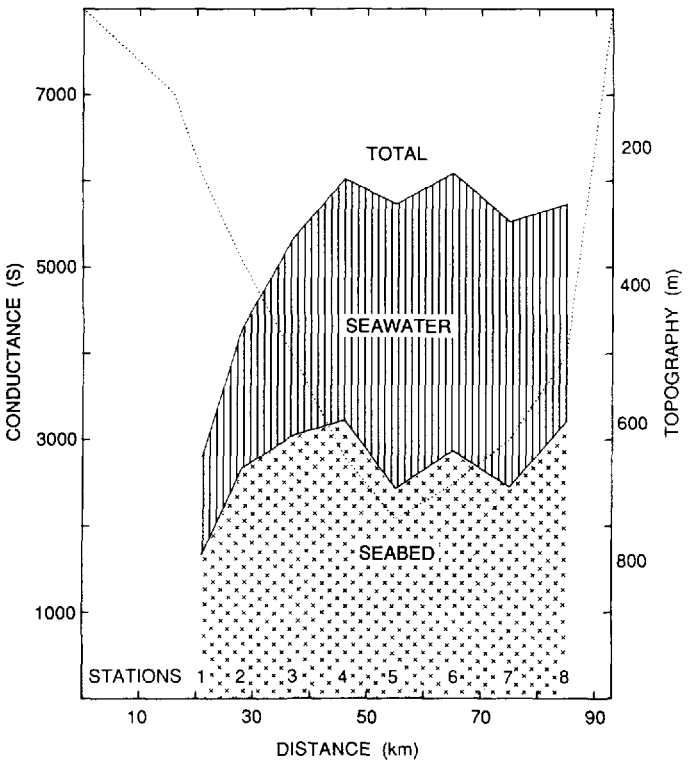

Figure 7. Transects of electrical conductances. The magnitudes and spatial patterns of seabed and seawater electrical conductances are compared by showing the median of the observed values at each site. Note the rather uniform pattern of seabed conductance from sites 2–8 and the marked reduction of seawater conductance compared with seabed conductance at the western end of the transect.

b. Estimating t from $\bar{v}^*$. The $T - \Delta\phi$ relationship (6) incorporates H_e through its lateral average ($\langle H_e \rangle$) and deviation (H_e'). If the nonlinearity in $\Delta\phi$ is unimportant, $\langle H_e \rangle$ is the constant that converts subcable voltages into volume transport. To reveal the likelihood of this situation, the accuracy of $\bar{v}^* \langle H_e \rangle$ for estimating t was assessed. Besides showing that $\bar{v}^* \langle H_e \rangle$ is an accurate estimate of t at all sites, Figure 9 shows that $\bar{v}^* \langle H_e \rangle$ is superior to $\bar{v} \langle H \rangle$, a more conventional estimate of t. A ramification of this finding is that, once $\langle H_e \rangle$ is known, accurate estimation of volume transport could be achieved with just a few horizontal electric field recorders, which would measure $\bar{v}^*$ (Lilley *et al.*, 1986). Looking at the data in Figure 9, one can see that the relative error of $\bar{v}^* \langle H_e \rangle$ decreases when it is laterally integrated. Hence the accurate estimation of t by $\bar{v}^* \langle H_e \rangle$ should be mirrored by their respective lateral integrals.

Figure 10 further quantifies the usefulness of $\bar{v}^*$ for estimating t. Two important conclusions from this regression are that $\bar{v}^*$ and t vary in direct proportion because the

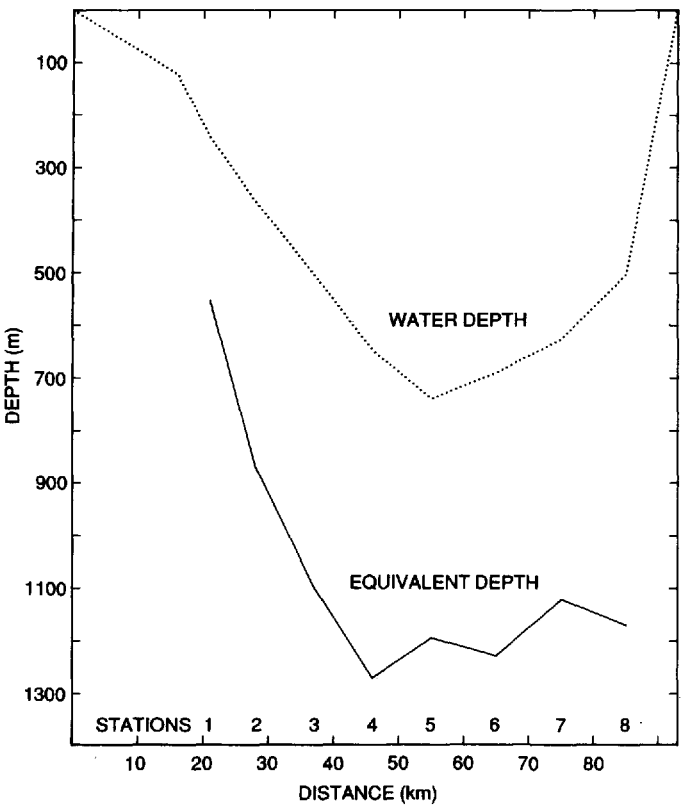

Figure 8. Transects of H_e and H. The greater magnitude and more uniform distribution of H_e compared with H is obvious in this figure, which displays the median of the observed values at each site. The difference between the two depths reflects the electrical conductance of the seabed.

intercept is effectively zero, and that t can be accurately predicted with $\bar{v}^*$ because the prediction error is 10% (Weisberg, 1980) and because 85% of t variability is explained by $\bar{v}^*$. The gradient (1134 m) in Figure 10 is an estimate of equivalent depth. This estimate of equivalent depth is 8% larger than the $\langle H_e \rangle$ of 1050 m reported by Larsen and Sanford (1985), probably because the profiling data set did not include shallow water regions where t was expected to be low (Fig. 2) and because the poor quality $\bar{v}^*$ estimates omitted from the regression were from shallower sites.

c. Calibration relation. The t and H_e data were used to evaluate the $T - \Delta\phi$ calibration (6). The lateral average of H_e values in Figure 8 ($\langle H_e \rangle$) was 1080 m, which agrees well with what Larsen and Sanford (1985) found. For each transect of simultaneous profiling measurements, the lateral average and deviations for t were computed. Then the nonlinear term $\langle t' H_e' \rangle / \langle H_e \rangle \langle t \rangle$ was evaluated. For all three

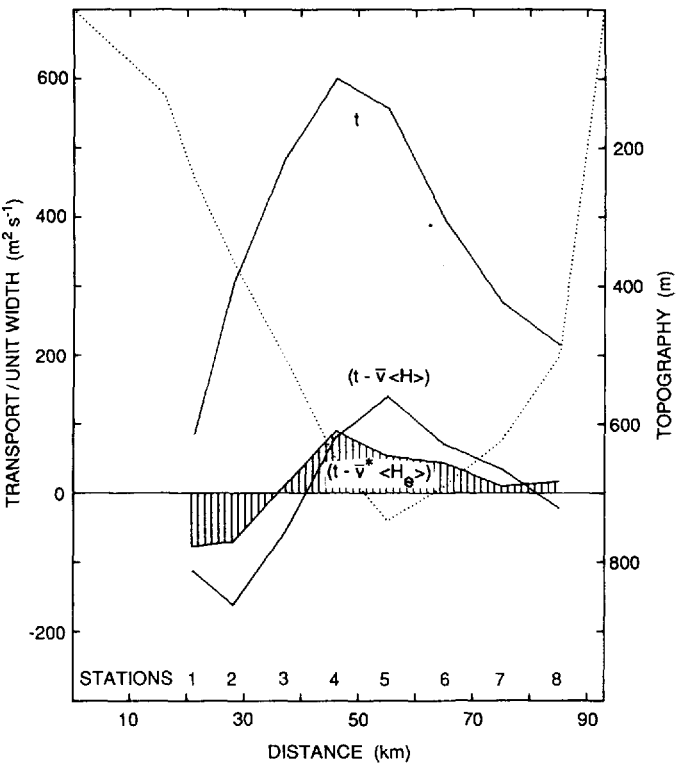

Figure 9. Estimating t with $\bar{v}^*\langle H_e\rangle$. The accuracy of estimating transport with $\bar{v}^*\langle H_e\rangle$ is compared with a more conventional estimate $\bar{v}\langle H\rangle$ by showing the residual after each was subtracted from the observed transport. The transport transect helps judge the relative error of $\bar{v}^*\langle H_e\rangle$. The median of the observed values at each site is shown.

profiling transects $\langle t'\ H_e'\rangle/\langle H_e\rangle\langle t\rangle$ was always about $+0.05$, which indicates a correlation between higher transport values and larger equivalent depths. Because $\langle t'\ H_e'\rangle/\langle H_e\rangle\langle t\rangle$ was small compared with unity, we concluded that $\Delta\phi$ and T will effectively vary in direct proportion.

Accordingly, the calibration relating subcable voltages to the volume transport of the Florida Current at 27N is

$$\text{Transport (sverdrups)} = 27 \times \text{Voltage (volts)}. \tag{7}$$

The calibration coefficient was obtained by inflating the $\langle H_e\rangle$ estimate (1080 m) by 5% to account for the observed nonlinear correction, and then dividing by F_z ($0.42\ 10^{-4}$ T). The adjusted coefficient matches the gradient of Figure 10. Transports derived from (7) will be accurate to ± 5–10%, figured from the accuracy of the regression in Figure 10.

One should not expect (7) to duplicate the calibration of Larsen and Sanford (1985);

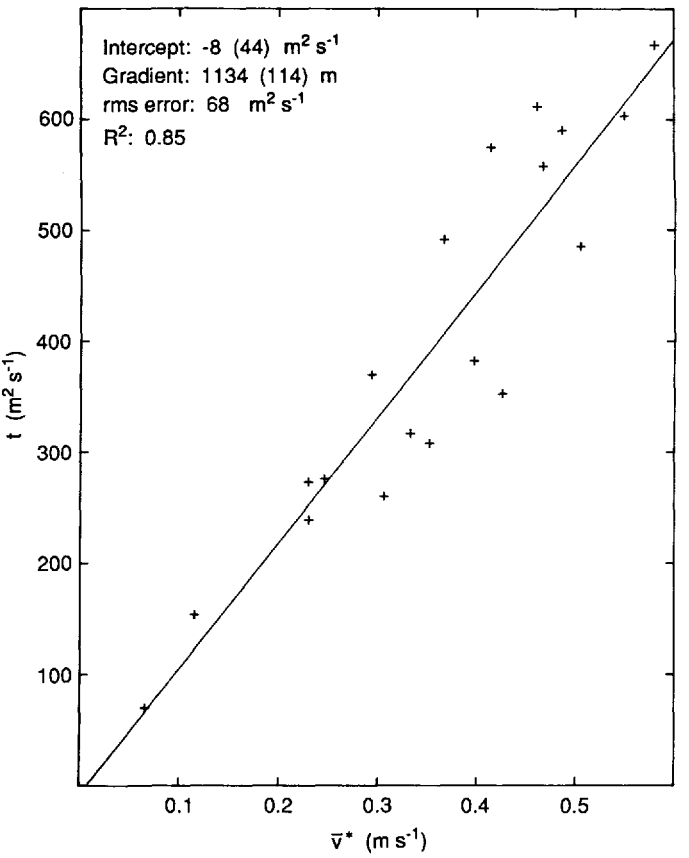

Figure 10. Simple linear regression between t and $\bar{v}^*$. The utility of $\bar{v}^*$ for estimating t is quantified in this figure using data taken along the transect at 27N. The gradient of the best-fit line drawn through the data is an estimate of H_e. Only profiles in which the data return exceeded 80% are included. Statistics for the regression are shown, with the standard error for each of the regression parameters in parentheses.

the subcable and profiling transects are not identical and, furthermore, we have ignored the shoal regions, thereby slightly biasing $\langle H_e \rangle$. We view Larsen and Sanford's (1985) result as the definitive calibration for the subcable between Jupiter and Settlement Point. The calibration coefficient in (7) is only 8% larger than their value. This good match between the two calibration relations provides encouraging support for our experimental approach.

At first sight (7) would seem to be valid only as long as the observed transport distributions are representative. But the utility of evaluating $H_e(x)$, which was the key to unraveling the nonlinearity in $\triangle\phi$, emerges again. Once $H_e(x)$ is known, the sensitivity of $\triangle\phi$ to any distribution of transport can be found, and the robustness of the linear calibration can be determined without a long term calibration program. As we

show in the Appendix, when the effects of realistic meandering of the Florida Current at 27N are assessed, the sensitivity of the voltages to meandering does not exceed 8%, which lies within the limits of accuracy of the calibration.

7. Discussion

Given that subcable voltages have had ambiguous interpretations elsewhere, the encouraging results in the northern Florida Straits prompt two questions.

- Why do voltages vary linearly with transport at this location?
- Why are the voltages largely unaffected by changes in the transport distribution, such as meandering?

The answers follow from examining the effects of the large magnitude and uniform distribution of $H_e(x)$ upon subcable voltages in the northern Florida Straits. Recall that in Section 3b the magnitude of H_e was shown to be the key to the linearity of subcable voltages, except where t and H_e tend to be uncorrelated. At 27N in the Florida Straits both effects are important.

The Florida Current transport is about twice the value inferred from uncalibrated subcable voltages observed near 27N, so only half of the generated (open-circuit) voltage is being observed (Sanford, 1982). Historically, such a reduction in voltage has always been attributed to seabed shorting because the nonlinearity in voltage could not be evaluated.

Based on (6), however, four explanations are possible:

$$\text{(I)}\quad \langle H_e\rangle = \langle H\rangle; \qquad \frac{\langle t'\,H'\rangle}{\langle H\rangle\langle t\rangle} = 0.5.$$

$$\text{(II)}\quad \langle H\rangle < \langle H_e\rangle < 2\langle H\rangle; \qquad 0 < \frac{\langle t'H'_e\rangle}{\langle H_e\rangle\langle t\rangle} < 0.5.$$

$$\text{(III)}\quad \langle H_e\rangle = 2\langle H\rangle; \qquad \frac{\langle t'H'_e\rangle}{\langle H_e\rangle\langle t\rangle} = 0.$$

$$\text{(IV)}\quad \langle H_e\rangle > 2\langle H\rangle; \qquad \frac{\langle t'H'_e\rangle}{\langle H_e\rangle\langle t\rangle} < 0.$$

While (IV) is unlikely because it requires the highest transport to be found over shoals and vice versa, and (I) could be assessed from a transect of t measurements, it is difficult to choose between (II) and (III) without knowing something about H_e and its spatial structure.

Our finding that $\langle H_e\rangle$ is about twice $\langle H\rangle$ (Fig. 8) provides strong support for (III). Moreover, this finding shows that subcable voltages will respond weakly to the transport distribution because the nonlinear part of the voltage is decreased fourfold compared with the value it would have if the seabed were insulating. In addition to its large magnitude, H_e is rather uniform for much of the transect, producing a low

covariance between t and H_e which further diminishes the sensitivity of voltages to the form of the flow. As the results of Larsen and Sanford (1985) show, the advantage of a weak response to the transport distribution can far outweigh the disadvantage of smaller voltage.

Our study provides some hints about what site characteristics suggest a suitable region for subcable measurements. Two advantageous qualities of an oceanic site are flat bottom topography and/or large and uniform seabed conductance. Moreover, horizontally confined flow and/or a uniform transport distribution will simplify interpreting the voltages. Finally, evaluating the covariance between water depth and transport may help to see whether voltages will vary directly with transport. The common effect of these characteristics is that they minimize the nonlinearity in the voltages.

Using the results from Section 6, we have learned why voltages reflect transport at 27N in the Florida Straits. We now discuss what we have learned about our experimental approach and the assumptions made in the theory.

The data in Figures 3 and 4 provide strong evidence that the experimental method was successful. The *barotropy* displayed by $\tilde{v}$, irrespective of flow speed and location (Fig. 3), matches what theory expects for this variable (Section 4a)—that it be depth invariant. The nonconstancy of $\tilde{v}$ at a given site is due to depth-dependent effects: measurement errors and higher order terms in $\partial\phi/\partial x$ (Section 3a). These depth-dependent contributions have no significant effect on $\tilde{v}$. Even more importantly, the $\bar{v}^*$ data derived from these $\tilde{v}$ observations are highly correlated with $\bar{v}$ (Fig. 4), corresponding to theory (see (3)) and substantiating two implicit assumptions in our data reduction that the "noise" in $\tilde{v}$ is both additive and site independent. This corroboration between theory and measurement suggests that not only has our experimental method been successful but that the assumptions in the theory are reasonable.

The validity of the assumptions underpinning (2), (5), and (6) can be examined with the data. Figure 3 provides striking observational confirmation that the induced electric field $(-F_z\bar{v}^*)$ is depth invariant. Second, the data in Figure 4 and the table in Section 5b support the assumption that depth-independent electric currents are absent or weak. These extraneous currents would enhance the scatter in a $\bar{v}^*$ versus $\bar{v}$ regression because their effect is spatially variable, depending on water depth. The high coefficient of determination (R^2) and low scatter displayed in Figure 4 belie such contamination. Furthermore, subcable voltages would include the effects of any extraneous electric currents. If such currents, rather than instrument error, were the difference between $\bar{v}^*$ and $\tilde{v}$, the concurrent subcable voltage would agree better with the integral of $F_z\tilde{v}$ than with the lateral integral of $F_z\bar{v}^*$. Such was not the case—the former integral overestimated subcable voltages by up to 25%. Finally, the data in Figure 8 show that $H_e'/\langle H_e\rangle < 1$ is a reasonable simplification except at site 1. This exception is unimportant because very little transport is found in the shallow water off Jupiter and, moreover, the largest uncertainty for H_e was found at this site.

In summary, the data provide strong evidence for the success of the measurement technique, the validity of the key assumptions, and the suitability of this site for monitoring transport with subcable voltages. We now use the results from Section 6 to discuss a few relevant hypotheses.

Larsen (1982) believes that a deep conducting earth must be included in any model of motional voltages in the northern Florida Straits. In his calculations, seafloor sediments are thought to be 1 km thick. Oilwell data tabulated by Manheim and Horn (1968) show that land sediments west of Jupiter are at least 3–4 km thick. If the thickness of seabed sediments off Jupiter reflects nearby land sediments, a canonical value for sediment conductivity of 1 S/m will adequately account for the seabed conductance (2800 S) in the Florida Straits.

Our results also verified the hypothesis of Sanford and Flick (1975) that transport and voltage are more linearly related over a highly conducting seabed. Although not the asymptotic limit they discussed, the large $\langle H_e \rangle$ observed at 27N still strongly reduces the nonlinearity of the subcable voltages. This effect was augmented by the low (t, H_e) covariance.

To quantify this idea a little, we compared the results of redistributing the transport observed at 27N over conducting and insulating seabeds. The mechanics of our approach are described in the Appendix. Over the insulating seabed, simulated by using $H_e = H$, the subcable voltages overestimated transport by 12% when the observed t values were shifted west by one site and underestimated by 9% for a similar eastward shift. The corresponding changes over conducting sediments were 5% and 7% respectively. So, if the transport core were to move as far as from site 5 to site 3 in the northern Florida Straits, which is about three times the rms variation reported by Olson *et al.* (1983), the subcable voltages would increase by 20% over an insulating seabed, but only by 12% over a conducting seabed. Hence the conducting seabeds have attenuated the sensitivity of the subcable voltages to meandering by 40%.

During this study some data were also collected in the central Florida Straits (Fig. 2) to examine the along-stream gradient of bottom conductance noted by Sanford (1982). Sanford and Schmitz (1971) reported that $\langle H_e \rangle$ had a value of 614 m off Miami. But at the northern end of the Florida Straits $\langle H_e \rangle$ is 1510 m, which was calculated from data tabulated by Sanford (1982). The $\langle H_e \rangle$ value found at 27N is 1080 m, which is bracketed by the $\langle H_e \rangle$ values found to the south and the north. Data from sites 4 and 10 were used to look for this gradient in H_e. In the table, σ_{H_e} is the standard error of H_e.

Station	H (m)	H_e (m)	σ_{H_e} (m)	Estimates
4	645	1271	75	4
10	755	1300	20	4

These results showed no statistically significant gradient in H_e between 27N (stn. 4) and 26.5N (stn. 10). How well the midstream value of H_e at station 10 reflects $\langle H_e \rangle$ is

unknown, but a uniform spatial gradient of bottom conductance between Miami and Fort Pierce would seem unlikely, based on these results.

Given the sudden change in H_e between the central Florida Straits (26.5N) and the Miami (26N) value, the results of this study cannot be accurately extrapolated to say anything about the seabed conductance at Key West. A separate study will be required to ascertain whether the old Key West to Havana cable data can be recalibrated in some way to make them useful, or whether the meandering over the shelf south of the keys makes the cable calibration just too nonlinear there.

8. Conclusions

In the northern Florida Straits, Florida Current transport can be accurately monitored with subcable voltages because transport magnitude is the dominant contribution to the voltage signal; voltages respond only weakly to changes in the transport distribution. Elsewhere, this secondary sensitivity of subcable voltages has caused their interpretation to be ambiguous. The weak response to the distribution of the Florida Current transport at 27N arises because seabed conductance is both large and rather uniform across most of the transect. This connection can be understood by considering the terms in (6). The observed pattern of seabed conductance is manifest as a large, flat equivalent water depth, H_e. Because this pattern is poorly correlated with transport, voltages are desensitized to the form of the flow. This weak sensitivity is further attenuated by the large magnitude of H_e, which normalizes the (t, H_e) covariance in (6).

We have introduced an experimental technique for analyzing how subcable voltages are constituted and for determining if and why they reflect volume transport. For oceanographic studies, two important benefits arise from this new approach. It ascertains the relationship between voltages and volume transport without requiring an existing cable and an extended calibration program. Second, the technique tests the sensitivity of the voltages to the spatial distribution of transport. Given the pressing need for observations to help understand seasonal and interannual variability in the ocean, the usefulness of subcable voltages should not be overlooked. The validity of their interpretation can now be assessed. Wherever subcable voltages are linearly related to transport, an accurate, cost-effective scheme is available for observing ocean currents over many years.

Acknowledgments. We gratefully acknowledge significant assistance from Bob Molinari, Pat McKeown, and George Maul during our work in the Florida Current. Bob Molinari and Kevin Leaman generously provided the PEGASUS data. Jimmy Larsen provided cable voltages for the times of XCP transects. This research was funded by the Office of Technology and Engineering Services of NOAA under grant NA81AA-D-00078 and the National Science Foundation under grant OCE-84-13234. This is contribution number 1673 of the University of Washington, School of Oceanography.

APPENDIX

Robustness of the $T - \triangle\phi$ calibration

The advantage of determining $H_e(x)$ for understanding and evaluating the nonlinearity of subcable voltages has been emphasized in this paper. Knowing $H_e(x)$ is also useful for analyzing the sensitivity of the voltages to realistic meandering of the Florida Current at 27N. Based on this analysis, an objective appraisal of the robustness of the linear $T - \triangle\phi$ calibration can be made without a long-term calibration program.

Although (7) was derived using only three transects of transport, its robustness under any distribution of transport can be evaluated via (6) because $H_e(x)$ is known. Several schemes would seem possible for exploring the robustness of the $T - \triangle\phi$ calibration.

- Evaluate the nonlinear term in (6) for each transport distribution and see how much its magnitude fluctuates.
- Estimate $\triangle\phi$ via (5) for each transport distribution, use (7) to predict T, and compare its value with the prescribed T.
- Compute a lateral average for H_e that is weighted by transport and see how much its value fluctuates with the distribution of transport.

But they are all equivalent as we now show.

Define $\langle H_e\rangle_t$ to be a transport-weighted harmonic mean value for equivalent depth

$$\frac{1}{\langle H_e\rangle_t} = \sum_{i=1}^{N} \frac{\alpha_i}{(H_e)_i},$$

where α_i is the fraction of the volume transport (T) found at site i, $(H_e)_i$ is the equivalent depth, and N is the number of sites across a transect. $(\triangle x)_i$ will be used below to describe the flow width represented by the datum measured at site i.

Eq. (5) can now be approximated as

$$\frac{\triangle\phi}{F_z} = \frac{T}{\langle H_e\rangle_t}. \tag{8}$$

By substituting

$$\alpha_i = \frac{t_i(\triangle x)_i}{T}; \quad t_i = \langle t\rangle + t_i'; \quad (H_e)_i = \langle H_e\rangle + (H_e')_i$$

in the right-hand side of (8), and simplifying as described in Section 3b, it follows that

$$\frac{1}{\langle H_e\rangle_t} = \frac{1}{\langle H_e\rangle}\left[1 - \frac{\langle t'H_e'\rangle}{\langle H_e\rangle\langle t\rangle}\right].$$

Thus we see that $\langle H_e \rangle_t$ both incorporates the nonlinearity in (6) and emerges from (5), thereby demonstrating the equivalence of the three approaches listed above.

The robustness of the linear $T - \triangle\phi$ calibration is now evaluated by synthesizing the subcable voltage. Then a simpler method, which exploits the uniform distribution of H_e, is shown to produce similar results. Based on these calculations, we conclude that (7) will be an accurate and robust calibration for converting subcable voltages into the volume transport of the Florida Current at 27N.

a. Evaluating $\triangle\phi$. Observed meandering of the cold "wall" of the Florida Current at 27N has a standard deviation of 7 km (Olson *et al.,* 1983). For each of the three profiling transects, observed t values were shifted west and then east by one station; the average station spacing is just less than 10 km. We simulated $\bar{v}^*$ by dividing the shifted t by the local H_e. The transects of simulated $\bar{v}^*$ were multipled by $\langle H_e \rangle$ (1080 m) and integrated to produce an estimate of volume transport that was then compared with the lateral integral of the t data.

When the transport field was shifted westward, the subcable voltages overestimated transport by 5%; for an eastward shift, the voltages underestimated the transport by 7%. From this test, we conclude that the calibration relation derived from the profiler data seems fairly insensitive to changes in the spatial distribution of transport. The voltages change by less than ±10% when realistic transport meandering is simulated.

b. Using $\langle H_e \rangle_t$. Looking at Figure 8, one can see that the spatial structure of equivalent depth at 27N can be reasonably approximated by a two-tier model. The step between the tiers was placed at site 2 and representative values for H_e were assigned to each level. East of site 2, the equivalent depth ($\langle H_e \rangle_{\text{deep}}$) was 1146 m, which is the median H_e value for the corresponding region in Figure 8. West of site 2, the equivalent depth ($\langle H_e \rangle_{\text{shallow}}$) was 600 m. This value approximates the few data observed in this region and is the transport-weighted difference between $\langle H_e \rangle_{\text{deep}}$ and the $\langle H_e \rangle$ value reported by Larsen and Sanford (1985). For this two-tier model,

$$\langle H_e \rangle_t = \frac{\langle H_e \rangle_{\text{deep}}}{(1 - \alpha_{\text{shallow}}) + \alpha_{\text{shallow}} \dfrac{\langle H_e \rangle_{\text{deep}}}{\langle H_e \rangle_{\text{shallow}}}},$$

where α_{shallow} is the fraction of T found over the upper tier. Because $\langle H_e \rangle_{\text{deep}} / \langle H_e \rangle_{\text{shallow}}$ is about 2 and $\alpha_{\text{shallow}} < 1$, this expression can be further simplified to

$$\langle H_e \rangle_t \approx \langle H_e \rangle_{\text{deep}} (1 - \alpha_{\text{shallow}}),$$

which emphasizes the transport weighting in $\langle H_e \rangle_t$. For the observed transects, $\alpha_{\text{shallow}} = 0.08$, whereas after the t data are shifted west by one site, $\alpha_{\text{shallow}} = 0.16$. On the other hand, after the t data are shifted east by one site, $\alpha_{\text{shallow}} = 0.03$. These numbers

suggest that $\langle H_e \rangle_t$ does not change by more than about 10% for realistic redistribution of the transport.

REFERENCES

Bowden, K. and P. Hughes. 1961. Flow of water through the Irish Sea and its relation to wind. Geophys. J. Roy. Astr. Soc., *5*, 265–291.

Chave, A. and C. Cox. 1982. Controlled electromagnetic sources for measuring electrical conductivity beneath the oceans. 1. Forward problem and model study. J. Geophys. Res., *87*, 5327–5338.

Firing, E., R. Lukas, J. Sadler and K. Wyrtki. 1983. Equatorial undercurrent disappears during 1982–83 El Niño. Science, *222*, 1121–1123.

Halkin, D. and T. Rossby. 1985. The structure and transport of the Gulf Stream at 73°W. J. Phys. Oceanogr., *15*, 1439–1452.

Larsen, J. 1982. Electromagnetic transport measurements of the Florida Current, *in* Proc. of the IEEE Second Working Conference on Current Measurement. Hilton Head, South Carolina. 19–21 January 1982, M. Dursi and W. Woodward, eds., 137–143.

Larsen, J. and T. Sanford. 1985. Florida Current volume transports from voltage measurements. Science, *227*, 302–304.

Lee, T., F. Schott and R. Zantopp. 1985. Florida Current: low-frequency variability as observed with moored current meters during April 1982 to June 1983. Science, *227*, 298–301.

Leetmaa, A., T. Rossby, P. Saunders and D. Wilson. 1980. Subsurface circulation in the Somali Current. Science, *209*, 590–592.

Lilley, F.E.M., J. Filloux, N. Bindoff, I. Ferguson and P. Mulhearn. 1986. Barotropic flow of a warm-core ring from seafloor electric measurements. J. Geophys. Res., *91*, 12,979–12,984.

Longuet-Higgins, M., M. Stern and H. Stommel. 1954. The electric field induced by ocean currents and waves, with applications to the method of towed electrodes. Papers in Physical Oceanography and Meteorology, M.I.T. and W.H.O.I., *XIII*, 1–37.

Malkus, W. and M. Stern. 1952. Determination of ocean transports and velocities by electromagnetic effects. J. Mar. Res., *11*, 97–105.

Manheim, J. and T. Horn. 1968. Composition of deeper subsurface waters along the Atlantic Continental Margin. Southeastern Geology, *9*, 215–236.

Molinari, R., G. Maul, F. Chew, D. Wilson, M. Bushnell, D. Mayer, K. Leaman, F. Schott, T. Lee, R. Zantopp, J. Larsen and T. Sanford. 1985. Subtropical Atlantic climate study: Introduction. Science, *227*, 292–294.

Olson, D., O. Brown and S. Emmerson. 1983. Gulf Stream frontal statistics from Florida Straits to Cape Hatteras derived from satellite and historical data. J. Geophys. Res., *88*, 4569–4577.

Rossby, H. T. 1969. A vertical profile of currents near Plantagenet Bank. Deep-Sea Res., *16*, 377–385.

Sanford, T. 1971. Motionally induced electric and magnetic fields in the sea. J. Geophys. Res., *76*, 3476–3492.

—— 1982. Temperature transport and motional induction in the Florida Current. J. Mar. Res., *40* (Suppl.), 621–639.

Sanford, T., R. Drever and J. Dunlap. 1978. A velocity profiler based on the principles of geomagnetic induction. Deep-Sea Res., *25*, 183–210.

—— 1985. An acoustic doppler and electromagnetic velocity profiler. J. Atmos. Ocean. Tech., *2*, 110–124.

Sanford, T., J. Dunlap, R. Drever and E. D'Asaro. 1981. Design, operation and performance of an Expendable Temperature and Velocity Profiler (XTVP). Technical Report, APL-UW 8110, Applied Physics Laboratory, University of Washington, Seattle, WA, 164 pp.

Sanford, T. and R. Flick. 1975. On the relationship between transport and motional electric potentials in broad, shallow currents. J. Mar. Res., *33,* 123–139.

Sanford, T. and W. Schmitz. 1971. A comparison of direct measurements and GEK observations in the Florida Current off Miami. J. Mar. Res., *29,* 347–359.

Schmitz, W. and W. Richardson. 1968. On the transport of the Florida Current. Deep-Sea Res., *15,* 679–693.

Spain, P., D. Dorson and T. Rossby. 1981. PEGASUS: A simple, acoustically tracked, velocity profiler. Deep-Sea Res., *28A,* 1553–1567.

Stommel, H. 1956. Electrical data from cable may aid hurricane prediction. Western Union Tech. Rev., *10,* 15–19.

—— 1965. The Gulf Stream, 2nd ed, University of California Press, Berkeley and Los Angeles, 248 pp.

Taft, B. 1972. Characteristics of the flow of the Kuroshio south of Japan, *in* Kuroshio, Physical Aspects of the Japan Current, H. Stommel and K. Yoshida, eds., University of Washington Press, Seattle, 517 pp.

Teramoto, T. 1971. Estimation of sea-bed conductivity and its influence upon velocity measurements with towed electrodes. J. Oceanogr. Soc. Japan, *27,* 7–18.

Weisberg, S. 1980. Applied Linear Regression, Wiley, NY, 283 pp.

Wertheim, G. 1954. Studies of the electrical potential between Key West, Florida, and Havana, Cuba. Trans. Amer. Geophys. Union, *35,* 872–882.

Received: *28 November, 1986;* revised: *15 June, 1987.*